Evaluation of three-dimensional kinematics of the distal portion of the forelimb in horses walking in a straight line

Henry Chateau, DVM; Christophe Degueurce, DVM, PhD; Jean-Marie Denoix, DVM, PhD

Objective—To develop a method that allows quantification of the 3 anatomic rotations in the digital joints of moving horses and measure these rotations when horses are walking in a straight line on a hard track.

Animals—4 healthy French Trotter horses.

Procedure—Triads of ultrasonic kinematic markers were surgically linked to the 4 distal segments of the digits of the left forelimb of each horse. Three-dimensional (3-D) coordinates of these markers were recorded in horses walking in a straight line. The three angles of rotation of each digital joint were calculated by use of a joint coordinate system as well as the 3-D orientation of the hoof and third metacarpal bone. A calibration procedure was developed to convert data from measurements within a technical coordinate system to data in relation to an anatomically relevant coordinate system.

Results—Precision of the method was 0.5°, and repeatability of the calibrations resulted in variations of 1.4°. Extrasagittal movements of the proximal and distal interphalangeal joints were obvious during landing because the impact of the hoof was on the lateral side. Mean ± SD extension of the proximal interphalangeal joint was 10.0 ± 2.5°.

Conclusions and Clinical Relevance—This study provides a description of the technical background, error analysis, and procedures used to measure the 3-D rotations of the 4 distal segments of the forelimb in walking horses. As a major result substantial involvement of the proximal interphalangeal joint in the sagittal and extrasagittal planes,should incline investigators and clinicians to consider the functional importance of this joint. (*Am J Vet Res* 2004;65:447–455)

Prevention of digital joint disorders and treatment of affected horses often involve exercise management (proscribed gait and movements) and therapeutic shoeing combined with the properties of training surfaces.[1-5] Because they are difficult to quantify, the actual effects of these treatments remain unclear because of a lack of scientific evidence. Kinematic analyses that use skin markers are insufficiently accurate to measure slight changes in the movements of the digital joints induced by these treatments. Displacement of the skin relative to the underlying bones renders the measurements nonrepresentative of the actual joint motion.[6,7] Additionally, these analyses are restricted to the measurement of flexion-extension movements in the sagittal plane, whereas in vitro studies[2,8-10] have documented the quantitative importance of extrasagittal movements (passive abduction-adduction and axial rotation) in the digital joints. Finally, there is a lack of knowledge of the biomechanical behavior of the **proximal interphalangeal joint (PIPJ)**. This joint has often been neglected in kinematic analysis of the digits in horses. Authors justify this shortcoming on the basis that the PIPJ is fairly immobile and could therefore be considered a rigid joint.[11,12] However, in vitro studies[8,13] and quasistatic radiographic studies[2,6,14] have documented sufficient mobility in this joint to raise doubts about the assumption that the PIPJ be considered a rigid joint during locomotion.

To enhance our knowledge of the **3-dimensional (3-D)** behavior of the distal portion of the forelimb, a method was needed to measure 3 anatomic rotations in the 3 digital joints. Spatial orientation of a bone entails the definition of an orthogonal frame, rigid with the bone and numerically described with respect to a given observer by use of an orientation matrix.[15] This has been applied in vitro on isolated forelimbs equipped with kinematic markers implanted in the cortical bone of the phalanges and third metacarpal bone. Effects of changes in the transverse[8,9] and sagittal[13] orientations of the foot were quantified while the limbs were loaded by use of a power press. The angles of flexion-extension, passive abduction-adduction, and axial rotation have been calculated by use of the principles of the joint coordinate system[16] applied to the digital joints of horses.[17] Those preliminary studies have documented the ability of the method to detect small changes in joint angles. However, in vitro studies cannot simply be extrapolated to in vivo conditions because the rate of loading and orientation of the limb during loading by a press cannot completely mimic the situation in live horses.[8] Thus, the objectives of the study reported here were to describe the technical background, error analysis, and procedures used to measure 3-D motions of the 4 distal segments of the forelimb in moving horses and quantify these movements when horses are walking in a straight line on a hard track.

Materials and Methods

Animals—Four healthy French Trotter geldings (mean ± SD, 6 ± 2 years old) that weighed 495 ± 40 kg and were

Received May 27, 2003.
Accepted August 11, 2003.
From the Unité Mixte de Recherche de Biomécanique et Pathologie Locomotrice du Cheval, Ecole Nationale Vétérinaire d'Alfort, 7 avenue du Général de Gaulle, 94704 Maisons-Alfort, France.
Supported by funds from the Haras Nationaux, the Institut National de la Recherche Agronomique, and the Ecole Nationale Vétérinaire d'Alfort.
The authors thank Jean-Louis Brochet, Dr. Géraldine Cassiat, Dr. Christophe Desbois, Christophe Hode, Frantz Pleignet, Gen. Jean-Yves Pringent, Col. Xavier Ribot, Dr. Céline Robert, Dr. Aziz Tnibar, and Jean-Paul Valette for technical assistance.
Address correspondence to Dr. Chateau.

Unauthenticated | Downloaded 10/03/22 08:51 AM UTC

158 ± 4 cm high at the top of the shoulders were used in the study. None of the horses had clinical abnormalities of the musculoskeletal system or abnormal findings during evaluation of radiographs of the digits of the forelimbs. The procedures used were reviewed and approved by the Animal Care Committee of the Direction des Services Vétérinaires—Val de Marne, France.

Farriery—The hooves of both forelimbs on each horse were trimmed by an experienced farrier; hooves were trimmed to a length deemed appropriate for that horse. The hooves of the forelimbs then were equipped with special shoes made of a support shoe and a removable shoe. This system allowed us to attach several therapeutic shoes without extensive shoeing of the hooves during experimental sessions. Three 6-mm threaded holes were made in the support shoe. The support shoe was nailed onto the hoof wall. Removable shoes were rigidly screwed onto the support shoe by use of 3 countersunk bolts. Because the thickness of the shoes was deliberately thin (6 mm), the weight of such a device was approximately 500 g. The removable shoe used in the study was a standard iron shoe (20 mm wide). Horses were shod with this shoe at least 5 days before the beginning of the experimental session.

Surgical procedure—Kinematic markers were linked with the underlying bones by use of intracortical pins. Horses were anesthetized for the surgery. A hole was drilled on the lateral cortex of the third metacarpal bone of the left forelimb, and a 4-mm intracortical pin[a] was screwed into this hole. The external tip of this pin was approximately 1 cm above the surface of the skin. The same procedure was performed for the proximal and middle phalanges. Radigrphs were taken to ensure that the pins were correctly implanted. For the distal phalanx, the tip of the pin was welded onto a plate that was screwed into the lateral hoof wall (**Fig 1**). Consequently, movements of the hoof wall relative to the distal phalanx were neglected. Postoperative medication consisted of analgesics (phenylbutazone, 2 mg/kg, PO, q 12 h) and antimicrobials (trimethoprim and sulfamethoxazole, 5 mg/kg, PO, q 8 h). Horses were allowed to convalesce for 3 days after surgery.

Kinematic devices—Kinematic devices (ie, triads) were affixed to the tip of the intracortical pins. These triads were made of an aluminium sleeve with 3 rods connected to 3 noncollinear kinematic markers (Fig 1). The sleeve of the triad and the triangular tip of the pin fit together rigidly and reproducibly by the use of 2 screws, which allowed for removal and replacement of the devices in the same orientation and position. Orientation of the 3 kinematic markers was determined on the basis of ergonomic considerations and to obtain the greatest distance between 2 markers without regard to the orientation relative to the underlying bones. Total weight of the kinematic devices (including markers) was approximately 10 g.

Recording procedures—Recording procedures were performed by use of an ultrasonic kinematic analysis system[b] with special software.[c] The measuring procedure was based on the determination of the spatial coordinates of miniature ultrasonic microphones (markers) whose position relative to a fixed system of 3 ultrasonic transmitters (reference unit) was derived from the time delay between the ultrasonic pulses by use of triangulation.[18] For each session, the 3-D coordinates of the microphones were recorded during the stance phase of the stride when a horse stepped approximately 1 m from 1 reference unit. For each horse, a minimum of 8 sessions was recorded at a sampling rate of 60 Hz.

Horses were led in a straight line on a hard (asphalt) track. Each horse walked at its own comfortable speed (range, 1.18 to 1.37 m/s; mean, 1.28 m/s). At the beginning and at the end of the session, the horses were subjected to a clinical examination to ensure that the intracortical pins did not induce lameness while walking.

Figure 1—Photograph of the distal portion of the left forelimb of a horse after insertion of intracortical pins and attachment of 3 noncollinear kinematic markers affixed to the tips of the pins. Pins were inserted in each digital segment for measurement of movements of the digital joints in the horse when walking in a straight line on a hard track.

Anatomic alignment of the axes—Because the orientation of the 3 kinematic markers on a triad was adapted on the basis of ergonomic considerations, there was not a direct relation between the position of the markers and the underlying bones. Thus, additional information was needed to estimate the spatial orientation of a bone-embedded frame related to the anatomic alignment of the bones.[15] At the end of the test sessions, a special calibrating device[d] that allowed us to determine the axes of an orthogonal frame defined by 3 ultrasonic microphones was aligned with the nominal anatomic axes of the bones. Orientation of this anatomic frame was adjusted to closely approximate the symmetry axes of the bones. This

Unauthenticated | Downloaded 10/03/22 08:51 AM UTC

special calibrating device was designed to lean against the dorsal aspect of the segment parallel to its longitudinal axis and was manually adjusted by an experienced operator to align dorsopalmar and lateromedial axes with symmetry axes of the bones.

Signal processing—The 3-D coordinates of the markers were exported into a software program.[e] Data were filtered by use of a second-order recursive Butterworth low-pass digital filter in both forward and reverse directions; a cut-off frequency of 20 Hz was used.

Computation of joint angles—For each of the 3 digital joints (ie, **metacarpophalangeal joint [MPJ]**, PIPJ, and **distal interphalangeal joint [DIPJ]**), the same computational protocol was used. To characterize movement of the distal segment relative to the proximal segment of each joint, 5 reference frames were defined. These were the **global reference frame (G-frame)** defined by the ultrasonic transmitters, the **technical reference frame of the proximal segment (Tp-frame)**, and the **technical reference frame of the distal segment (Td-frame)**. The Tp-frame and Td-frame were defined by the bone-embedded triads during the test sessions. Calibrating steps allowed us to define the **anatomic reference frame of the proximal segment (Ap-frame)** and the **anatomic reference frame of the distal segment (Ad-frame)**. The reference frames were orthogonal right-hand coordinate systems determined by use of 3 kinematic markers.

The **unit vector associated with the *z*-axis of the anatomic reference frame** (k_A) was parallel to the nominal longitudinal axis of the corresponding bone, with the positive direction pointing in a proximal direction. The **unit vector associated with the y-axis of the anatomic reference frame** (j_A) was oriented laterally and parallel to the nominal mediolateral axis of the bone, and the **unit vector associated with the x-axis of the anatomic reference frame** (i_A) was directed dorsally, perpendicular to the 2 other axes and parallel to the nominal dorsopalmar axis of the bone **(Fig 2)**. Because only rotational information was needed, the location of the origin of the anatomic reference frame was not a concern, but orientation of the axes of the anatomic reference frame with respect to each of the bones was essential.

Considering that $[^{Ap}R_{Ad}]$ is a 3 × 3 rotation matrix that contains rotational information of the Ad-frame with respect to the Ap-frame, the final computation of the attitude of the Ad-frame with respect to the attitude of the Ap-frame was achieved by use of the following equation:

$$[^{Ap}R_{Ad}] = [^{Ap}R_{Tp}] \bullet [^{Tp}R_{G}] \bullet [^{G}R_{Td}] \bullet [^{Td}R_{Ad}]$$

where $[^{Ap}R_{Tp}]$ is the constant rotation matrix that related the Tp-frame to the Ap-frame and $[^{Td}R_{Ad}]$ is the constant rotation matrix that related the Ad-frame to the Td-frame (both of these matrices were initially calculated by use of the calibration recordings), $[^{G}R_{Td}]$ is a rotation matrix determined at each time interval on the basis of the position vectors of the kinematic markers measured for the Td-frame in the G-frame during the tests sessions, and $[^{Tp}R_{G}]$ is a rotation matrix determined at each time interval on the basis of the position vectors of the kinematic markers measured for the G-frame in the Tp-frame during the tests sessions. The effects of the sequence of matrix multiplication involved in this equation were depicted schematically (Fig 2).

The kinematics of each joint, which was contained in the matrix $[^{Ap}R_{Ad}]$, was resolved in accordance with the convention of the joint coordinate system[16] applied to the digital joints of horses.[17] In this cardonic system, the rotation matrix [R] was calculated by the use of the following sequence of rotations:

$$[R] = [R_F] \bullet [R_C] \bullet [R_R]$$

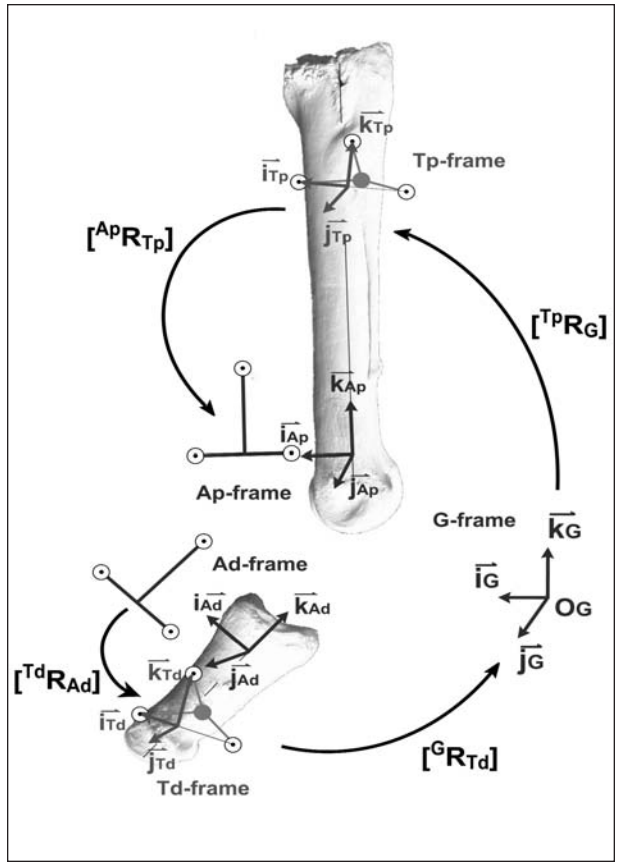

Figure 2—Diagram of the transformations used to obtain the orientation of the proximal phalanx (distal anatomic reference frame) with respect to the third metacarpal bone (proximal anatomic reference frame). Orientations of the technical reference frame of the proximal segment (Tp-frame) and the technical reference frame of the distal segment (Td-frame) in the global reference frame (G-frame) were determined during the test sessions, whereas their constant orientation relative to their respective anatomic reference frames (anatomic reference frame of the proximal segment [Ap-frame] and the anatomic reference frame of the distal segment [Ad-frame]) were obtained during calibration steps. Each reference frame was defined with 3 orthogonal unit vectors: i, j, and k. Indexes Tp, Ap, G, Td, and Ad referred respectively to Tp-frame, Ap-frame, G-frame, Td-frame, and Ad-frame. $[^{Ap}R_{Tp}]$ = Rotation matrix that related the Tp-frame to the Ap-frame. $[^{Td}R_{Ad}]$ = Rotation matrix that related the Ad-frame to the Td-frame. $[^{G}R_{Td}]$ = Rotation matrix that related the Td-frame to the G-frame. $[^{Tp}R_{G}]$ = Rotation matrix that related the G-frame to the Tp-frame.

where $[R_F]$ indicates flexion-extension rotation, $[R_C]$ indicates collateromotion (passive abduction-adduction), and $[R_R]$ indicates internal-external rotation. This meant that flexion-extension was measured around the y-axis of the proximal anatomic reference frame, axial rotation was measured around the z-axis of the distal anatomic reference frame, and collateromotion was measured around the x′-floating axis perpendicular to the other 2 axes **(Fig 3)**. The concept of collateromotion, established by a previous investigator,[2] was used to describe the passive abduction-adduction movements because there is no abductor or adductor muscle inducing these movements in the distal portion of the forelimb. A lateromotion (or passive abduction) is a rotation in the frontal plane of the distal segment in a lateral direction. Mediomotion, on the other hand, describes the opposite phenomenon (passive adduction). The joint coordinate system described here resulted in lateromotion (passive abduction)

Unauthenticated | Downloaded 10/03/22 08:51 AM UTC

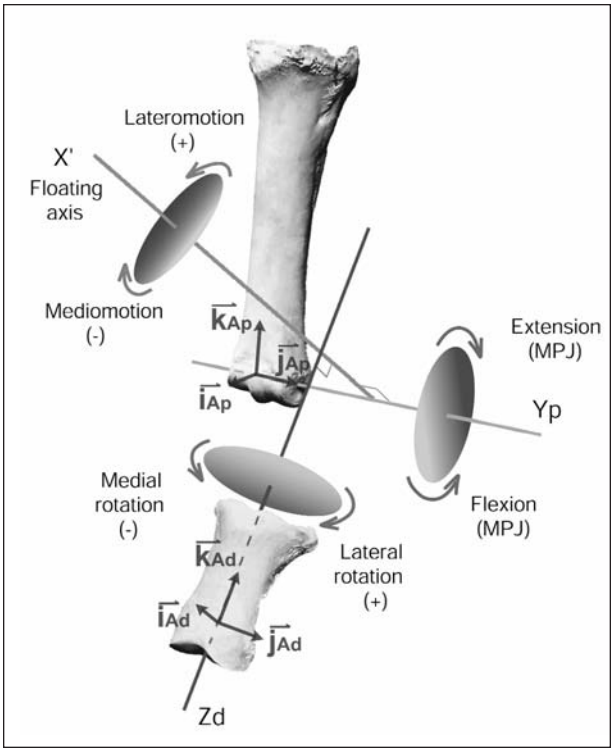

Figure 3—Schematic representation of a joint coordinate system for the metacarpophalangeal joint (MPJ) of the left forelimb of a horse. Rotations of the proximal phalanx relative to the third metacarpal bone are measured around the 3 axes (ie, Yp, X′, and Zd) of this system. – = Negative motion. + = Positive motion.

and lateral rotation as positive motions. The palmar joint angle of the DIPJ and PIPJ and the dorsal joint angle of the MPJ were used to describe flexion and extension such that flexion of the MPJ was positive motion whereas flexion of the DIPJ or PIPJ was negative motion.

Computation of attitude angles—The attitude angles of the anatomic reference frames of the hoof and third metacarpal bone were calculated relative to the G-frame. The attitude angles were defined as follows: pitch (inclination in the sagittal plane), roll (inclination in the frontal plane), and yaw (vertical rotation) of the segments. These angles were calculated by use of the cardonic system, with pitch angle measured around the y-axis of the anatomic reference frame of the corresponding segment, yaw angle measured around the vertical axis of the G-frame, and roll angle measured around the x′-floating axis perpendicular to the other 2 axes. For the hoof, the pitch angle was the angle between the toe line and the z-axis of the G-frame. This convention assigned backward rotation, lateral inclination, and medial rotation as positive motions. Yaw angle of the third metacarpal bone was not investigated because the large amount of inclination of this segment in the sagittal plane led to misinterpretation of the rotation of this segment around the z-axis of the G-frame.

Statistical analysis—Angle-time diagrams were plotted by use of analytic software.[e] Maximum and minimum values of the flexion-extension angles for the MPJ, PIPJ, and DIPJ were semiautomatically detected by use of derived curves. Attitude angles of the hoof were used to detect events of the stance phase. The stance phase was divided into 3 periods: landing, from initial impact of the hoof to hoof stabilization; bearing phase (ie, strict stance phase), from hoof stabilization to heel off; and breakover, from heel off to toe off. Initial impact of the hoof was detected by crosschecking 2 variables (beginning of the forward rotation of the hoof following heel impact and beginning of the medial rocking motion of the hoof following lateral quarter impact). The bearing phase was defined as the period of the stride when pitch, roll, and yaw angles of the hoof were invariable (ie, their derived curves were equal to zero). The breakover began at heel off, when the pitch angle of the hoof began to decrease (beginning of the forward rotation of the hoof), and ended at toe off, when the velocity of the pitch angle increased. The midstance phase of the stride was defined as the period when the third metacarpal bone was oriented vertically in the sagittal plane.[19]

An ensemble average of all strides for all horses was used to plot average angle curves. Time was expressed as a percentage of the stance phase from impact to toe off. Mean, SD, within-subject variability, and between-subject variability were calculated for each angle value. Ranges of motion were calculated, and the bounds of this interval were compared by use of an ANOVA to test the difference between initial and final values.

Precision of the method—Precision of the method was evaluated on the basis that the distances among the 3 ultrasonic microphones of a triad are theoretically invariable. The SD of angles and distances between the markers of each triad were calculated at each time point for each test session.[17,20]

Repeatability of alignment of the axes—Repeatability of the anatomic calibration step was also evaluated. Five calibrations performed on the same horse were used to measure the 9 joints angles of the same test session. Overall SD of the joints angles was calculated during the entire stance phase of the test session by use of the 5 calibrations.

Consistency of the anatomic axes—Anatomic calibrations were performed by use of a calibrating device adjusted by an experienced operator. To test the validity of this procedure, 1 of the horses was euthanatized after the experiments and the left forelimb of that horse was removed. Each digital bone (with its corresponding pin) was then separated from the surrounding soft tissues. The triads were replaced on the tip of the pins in the same orientation and position. A new calibration step was then performed in vitro on the bony segments. This procedure allowed us to improve the definition of the anatomic axes. In vitro and in vivo calibrations were then compared. Differences in the resulting joint angles were calculated at each time point of the stance during 1 test session. Mean ± SD of these differences was calculated during the entire stance phase.

Results

Error analysis—The precision calculation resulted in an overall SD of 0.3 mm for the distance measurements and 0.5° for the angle measurements. Overall mean SD (all joints and all angles) resulting from the 5 calibrations was 1.4° (**Table 1**). Use of in vivo or in vitro calibration resulted in differences that were < 3.1° for the angles of flexion-extension and ranged between 1.3° and 7.5° for extrasagittal angles. The SDs of these differences during the entire stance phase were small (< 0.6°), indicating that the differences resulted in a constant shift of the value with a preserved angle-time pattern.

Kinematics of the hoof and third metacarpal bone—Pitch angle of the hoof decreased significantly during landing corresponding to a forward rotation of the hoof (mean ± SD, –4.9 ± 5.5°; **Table 2**). This movement was variable between horses

Unauthenticated | Downloaded 10/03/22 08:51 AM UTC

(between-subject variability, 5.2°) and among test sessions for the same horse (within-subject variability, 3.2°). Roll angle of the hoof decreased significantly during landing (–7.1 ± 2.7°). For the 4 horses, the hoof hit the ground on its lateral side. This lateral impact was followed by a sudden medial rocking motion of the hoof that preceded hoof stabilization. During breakover, the hoof underwent a forward rotation associated with a lateral rocking motion and lateral rotation.

Sagittal verticality of the third metacarpal bone (midstance) was detected at 35.3 ± 3.6% of the stance phase. Roll angle of the third metacarpal bone was an indication of the global angle of abduction-adduction of the limb. When the hoof hit the ground, the limb was adducted. During the stance phase, the limb underwent abduction and was consequently abducted at take off. Mean amplitude of this abduction was 13.6 ± 4.1° from initial impact to toe off (Table 2).

Temporal variables—Mean ± SD duration of the stance phase from initial impact to toe off was 840.6 ± 80.1 milliseconds (**Table 3**). Landing was 7.4 ± 1.8% of the stance phase, and breakover was 9.9 ± 1.7% of the stance phase.

Range of motion of the MPJ—Mean ± SD maximum extension of the MPJ was at 39.7 ± 3.3% of the stance phase and reached 136.8 ± 2.6° (**Table 4**). A second peak for extension of the MPJ was detected in 1 horse. We did not detect a particular pattern for col-

Table 1—Error analysis to determine repeatability of the calibration and comparison between calibrations performed in vivo or in vitro on isolated bony segments of the distal portion of the left forelimb

	Mean of the SDs resulting from 5 calibrations during an entire stance phase			Mean ± SD differences resulting from in vivo or in vitro calibrations during an entire stance phase		
Joint	**F-E (°)**	**C (°)**	**AR (°)**	**F-E (°)**	**C (°)**	**AR (°)**
MPJ	1.4	1.3	1.5	1.6 ± 0.06	4.9 ± 0.55	7.5 ± 0.39
PIPJ	0.5	1.6	1.5	3.1 ± 0.01	3.8 ± 0.01	3.1 ± 0.04
DIPJ	1.9	1.5	1.3	2.2 ± 0.06	1.3 ± 0.60	2.3 ± 0.46
Mean	1.2	1.5	1.4	2.3 ± 0.04	3.3 ± 0.39	4.3 ± 0.30

F-E = Flexion-extension. C = Collateromotion. AR = Axial rotation. MPJ = Metacarpophalangeal joint. PIPJ = Proximal interphalangeal joint. DIPJ = Distal interphalangeal joint.

Table 2—Range of motion (ROM) of the attitude angles of the hoof and third metacarpal bone (MC3) for the left forelimb of 4 horses walking in a straight line on a hard track

		Pitch angle (°)				Roll angle (°)				Yaw angle (°)			
Segment	**Period**	**ROM**	**WSV**	**BSV**	**SD**	**ROM**	**WSV**	**BSV**	**SD**	**ROM**	**WSV**	**BSV**	**SD**
Hoof													
	Landing	–4.9*	3.2	5.2	5.5	–7.1*	2.3	1.6	2.7	–0.5	3.4	1.9	3.6
	Bearing	–0.1	0.8	0.5	0.9	–1.0	1.5	1.4	0.7	–0.1	0.7	0.5	0.9
	Breakover	–9.9*	2.3	2.2	2.9	1.6*	1.4	1.4	1.8	–2.9*	3.2	4.9	5.3
MC3													
	Stance	–51.6*	2.1	4.5	4.4	–13.6*	2.2	4.0	4.1	—	—	—	—
	Damping	–17.2*	1.5	2.8	2.9	–2.8*	1.4	0.9	1.8	—	—	—	—
	Propulsion	–24.7*	1.2	2.8	2.7	–7.5*	1.5	2.1	2.2	—	—	—	—

*Value differs significantly ($P < 0.05$) between the beginning and end of the period.
WSV = Within-subject variability. BSV = Between-subject variability. Landing = Period of stance phase from initial impact to hoof stabilization. Bearing = Period of stance phase from hoof stabilization to heel off. Breakover = Period of stance phase from heel off to toe off. Stance = Entire stance phase from initial impact to toe off. Damping = Period of stance phase from hoof stabilization to midstance. Propulsion = Period of stance phase from midstance to heel off. — = Not determined.

Table 3—Temporal variables for stride events and joint events during the stance phase for the left forelimb of 4 horses walking in a straight line on a hard track

		Time (%)*				Time (ms)			
Variable	**Event**	**Mean**	**WSV**	**BSV**	**SD**	**Mean**	**WSV**	**BSV**	**SD**
Stride									
	Hoof stabilization	7.4	1.1	1.6	1.8	61.3	8.0	12.1	14.0
	Midstance	35.3	2.5	3.5	3.6	296.4	19.9	36.5	37.4
	Heel off	90.1	1.3	1.4	1.7	757.3	25.6	80.7	74.4
	Toe off	100.0	0.0	0.0	0.0	840.6	32.9	85.6	80.1
Joint									
	MPJ-ME	39.7	3.4	1.1	3.3	333.3	33.1	25.7	37.9
	PIPJ-MF	13.7	2.9	3.5	4.1	113.8	23.9	22.7	30.2
	PIPJ-ME	93.4	3.3	1.6	3.5	784.4	44.3	66.4	71.8
	DIPJ-MF	20.0	3.5	4.1	5.1	167.7	26.5	41.1	45.2
	DIPJ-ME	97.6	2.2	2.4	2.9	819.9	31.3	77.4	74.5

*Percentage of the duration of the stance phase.
MPJ-ME = Maximum extension of the MPJ. PIPJ-MF = Maximum flexion of the PIPJ. PIPJ-ME = Maximum extension of the PIPJ. DIPJ-MF = Maximum flexion of the DIPJ. DIPJ-ME = Maximum extension of the DIPJ.

Unauthenticated | Downloaded 10/03/22 08:51 AM UTC

Table 4—Range of motion of the digital joints of the left forelimb of 4 horses walking in a straight line on a hard track

		F-E (°)				Collateromotion (°)				Axial rotation (°)			
Joint	Period	ROM	WSV	BSV	SD	ROM	WSV	BSV	SD	ROM	WSV	BSV	SD
MPJ													
	Landing	–10.8*	2.7	2.6	3.4	–0.5	1.6	0.5	1.6	0.6	1.8	1.1	2.1
	Bearing	0.2	3.5	0.6	3.4	0.1	0.5	0.1	0.5	0.0	1.5	1.8	2.2
	MPJ ext	–27.6*	2.6	2.7	3.3	–0.7	3.4	1.1	3.3	1.9*	1.6	1.5	2.1
	MPJ flex	24.9*	1.6	2.9	3.1	0.6	0.7	1.7	1.5	–1.8*	0.7	1.4	1.4
	Breakover	7.8*	1.6	1.0	1.8	0.2	0.4	0.6	0.6	–0.5*	0.4	0.1	0.4
PIPJ													
	Landing	0.9	1.5	1.3	1.8	0.2	2.2	1.0	2.3	–2.7*	2.0	1.9	2.6
	Bearing	9.0*	0.9	2.3	2.3	0.1	0.9	0.7	1.0	0.9*	1.1	1.5	1.7
	PIPJ flex	–0.9*	0.6	0.8	0.9	0.2	0.9	0.4	0.9	0.0	0.6	0.4	0.7
	PIPJ ext	10.0*	1.0	2.4	2.5	–0.1	0.8	0.5	0.9	0.9*	1.0	1.2	1.4
	Breakover	–0.3	0.6	0.6	0.8	0.4	0.6	0.3	0.6	1.2*	0.9	1.3	1.4
DIPJ													
	Landing	–12.9*	1.7	2.2	2.5	1.6*	2.4	0.5	2.5	–1.9*	1.7	0.3	1.6
	Bearing	34.4*	2.9	3.6	4.2	–2.2*	1.3	1.1	1.7	–2.8*	2.2	1.8	2.7
	DIPJ flex	–16.4*	1.7	2.9	3.1	0.8	2.1	0.9	2.1	–2.3*	1.7	0.8	1.7
	DIPJ ext	42.4*	1.7	4.7	4.4	–1.8*	1.0	1.2	1.6	–0.4	1.2	0.7	1.3
	Breakover	4.5*	1.9	1.9	2.5	–0.5	1.0	0.6	1.1	2.0*	1.2	1.5	1.8

MPJ ext = Period of the stance phase from initial impact to MPJ-Me. MPJ flex = Period of stance phase from MPJ-ME to toe off. PIPJ flex = Period of the stance phase from hoof stabilization to PIPJ-MF. PIPJ ext = Period of the stance phase from PIPJ-MF to heel off. DIPJ flex = Period of the stance phase from initial impact to DIPJ-MF. DIPJ ext = Period of the stance phase from DIPJ-MF to toe off.
See Table 1 and 2 for remainder of key.

lateromotion of the MPJ during the stance phase for horses walking in a straight line. Lateral rotation of the proximal phalanx relative to the third metacarpal bone was measured during extension of the MPJ, and medial rotation was detected during flexion of the MPJ.

Range of motion of the PIPJ—During landing, the PIPJ underwent slight extension, but the amplitude of this movement was significant for only 1 horse (Table 4). Flexion of the PIPJ was immediately after hoof stabilization, and maximum flexion of the PIPJ was at 13.7 ± 4.1% of the stance phase. This movement was brief and slight in walking horses (Table 4). The PIPJ underwent extension during the remainder of the stance phase. This movement reached its maximum at 93.4 ± 3.5% of the stance phase, which was not significantly different from the time at heel off. Mean amplitude of this extension was 10.0 ± 2.5° (range, 8.4° to 13.5°).

We did not detect a significant pattern in collateromotion for the PIPJ. Medial rotation of the second phalanx relative to the proximal phalanx was evident during landing, concurrent with the medial rocking motion of the hoof. During breakover, lateral rotation of the PIPJ accompanied lateral rocking motion and lateral rotation of the hoof.

Range of motion of the DIPJ—During landing, the DIPJ underwent sudden flexion. After hoof stabilization, the DIPJ continued to flex but at a slower rate. Mean ± SD maximum flexion was at 20.0 ± 5.1% of the stance phase and reached 160.4 ± 6.8°. Then the DIPJ underwent an extension until 97.6 ± 2.9% of the stance phase.

During landing, the DIPJ underwent lateromotion and medial rotation, concurrent with medial rocking motion of the hoof. After hoof stabilization, the DIPJ underwent slight mediomotion as well as lateral rotation during breakover.

Discussion

An ultrasonic kinematic analysis system was used to calculate the real-time 3-D coordinates of kinematic markers. Precision of this system was tested in a preliminary study.[18] Near reflective surfaces, disruptive ultrasound induced some systematic errors (approx 0.2°), but these were minimized when the experimental field was large (especially in outside conditions). In standard laboratory conditions, the precision was ± 0.1 mm and ± 0.2° for the distance and angle measurements, respectively.[18] In the study reported here, the precision calculation resulted in an overall SD of 0.3 mm and 0.5° for distance and angle measurements, respectively. These differences (decrease of precision in vivo, compared with precision of immobile markers for in vitro laboratory conditions) can be attributed to external disruptive conditions (eg, wind or artifacts) and possible vibrations of the ultrasonic microphones during the stance phase.

Nevertheless, the precision of this method was better than that for a photogrammetric method used in the same experimental recording field.[17] The main drawback of the kinematic analysis system was the need for a cable between the horse and measurement unit. This restricts experiments to slow gaits on a track or to treadmill examinations.

Methods and technical choices used in the study reported here were based on a method developed on isolated forelimbs.[17] Technical adaptations were needed to fit in vivo experiments.

Complete joint motion can be described by use of 3 degrees of freedom in rotation and 3 degrees of freedom in translation. The chosen model was deliberately limited to 3 degrees of freedom in rotation. Although translations have been qualitatively documented in vitro in digital joints,[2] the in vivo assessment of these movements was not within the scope of our study. Rotations are independent of translations,[21] and the

Unauthenticated | Downloaded 10/03/22 08:51 AM UTC

choice to study only rotations has no bearing on the results.[17] Joint motion was described as the movement of the distal segment relative to the proximal segment. The angle computation was chosen on the basis of recommendations of the International Society of Biomechanics.[22] These computations involved a joint coordinate system in which there was rotation about 1 axis of the local reference frame of the proximal segment, rotation about 1 axis of the local reference frame of the distal segment, and rotation about an intermediate axis (also called the floating axis) that was perpendicular to the other 2 axes.[16,22,23] The 2 segment-fixed axes (ie, the sequence of successive rotations) were chosen on the basis of results of another study[17] in which investigators tested the effects of 6 combinations for the digital joints of horses.

Spatial orientation of a bone entails definition of an orthogonal frame that is rigid with the bone.[15] Movement of surface markers affixed to the skin may not represent the actual movement of the underlying bone because of soft tissue deformation and may result in large artifacts that counteract the rigid-body theory.[24] In 1 study,[6] investigators measured skin displacement at the distal condyle of the proximal phalanx and determined that there were large movements of the skin in the digital area.

To avoid the problem of surface markers,invasive markers can be used for direct measurement of skeletal motion. This technique provides the most accurate means for determining bone movements.[25] Several kinematic studies[26-28] have used bone pins implanted in humans. In those studies, none of the subjects reported pain or substantial discomfort during the experiments. Bone pins have also been used in horses.[7,20,29] Steinmann pins implanted in a 6-mm canal drilled through the bone, including the bone cortex, do not affect locomotion of horses.[7] In the study reported here, clinical examination of the horses before and after the experiments did not reveal lameness induced by the pins.

Special attention was paid to establish reliable and reproducible anatomic coordinate systems consistent with functional and clinical terminology. Technical bone-embedded frames provided by the triads data did not have the aforementioned characteristic because their orientation was based only on experimental requirements.[15] The anatomic axes were obtained by use of a calibrating device that provided visible axes aligned with the bones.

Other methods are available to determine anatomic axes. Among these is external location of palpable anatomic landmarks by use of a pointer.[15] Provided that these anatomic landmarks are easily and reproducibly palpable, this method can enhance reproducibility of the calibration. However, palpable anatomic landmarks are not necessarily in the best location to reproduce axes of symmetry of the bones. This can result in increasing alignment problems of the anatomic frames and subsequent cross-talk,[28] especially for the middle phalanx, which is short and partly covered by the hoof with few easily palpable anatomic landmarks. When 2 landmarks used to determine the orientation of a frame axis are a short distance apart, macroscopic inaccuracies increase for this orientation.[15] As suggested in 1 study,[15] the involved landmarks could be calibrated simultaneously by use of a devise, which would make the orientation of the relevant axis visible to the operator. In the distal portion of the forelimb of horses, it was easier to adjust the orientation of a visible axis than to symmetrically locate landmarks that were barely palpable.

Anatomic calibration may also be performed by use of roentgen-stereophotogrammetric X-rays.[26,27,30] Anatomic landmarks can be identified with precision with this technique,[25] but the choice of the axes remains intricate, and the method is difficult to apply in live horses.[31]

In the study reported here, repetition of anatomic calibrations resulted in a mean inaccuracy in alignment of the axes of 1.4°, which was considered acceptable when compared with the results from another study[32] in which investigators tested the sensitivity of angles to an incorrect determination of the orientation of the flexion-extension axes in the knees of humans. However 2 conditions can be accurately compared only when the angles are calculated by use of the same calibration recording.

Finally, comparison of the results of the same test session calibrated in vivo or in vitro on isolated bony segments revealed that the maximum difference in the resulting angle of flexion-extension was 3.1°. This difference reached 7.5° for the angle of axial rotation of the MPJ. Bony segments are not parallelepipeds, and a normal coordinate system can only approximate nominal symmetry axes of the bones. Interestingly, the differences in joint angles resulting from calculations with in vivo or in vitro calibrations had few variations during the stance phase, documenting that in vivo calibration shifted to some extent the absolute value of angles, compared with in vivo calibration, but preserved the pattern of joint motion. For this reason, differences in the shape of the movements were reported rather than the absolute positions (ie, range of motion and relative values rather than absolute values).

For ethical reasons, it was decided that we should limit the number of subjects in the study. Only 4 horses were used. Therefore, even when patterns of motion were extremely similar for these 4 horses, generalization of the results should be considered with some caution.

Because the study reported here was part of a larger study, special shoes were designed to compare several therapeutic shoes without taking the nails out of the hoof. Special attention was paid to prevent the shoes from being too thick or too heavy. Shoes in this system weighed approximately 500 g. The effects of shoeing and shoe weight on the distal portion of a limb on gait quality have been studied in horses during trotting,[33] and it was revealed that primarily variables in the swing phase were affected at high speed. Thus, the study reported here was limited to the analysis of the stance phase at a slow gait.

Kinematic analysis of sagittal inclination of the hoof (pitch angle) has been evaluated in horses during walking and trotting.[4,34,35] Analysis of results of the study reported here confirmed that the sagittal inclina-

Unauthenticated | Downloaded 10/03/22 08:51 AM UTC

tion of the hoof at landing was variable between and within horses. In most cases, the hoof was positioned with the heel lower than the toe, and the heel touched down first, followed by a forward rotation of the hoof during landing. In other cases, the toe and the heel were horizontally aligned during landing. This movement has been described as a flat-footed impact in a study[34] in which the investigator used sagittal plane kinematics. However, 3-D analysis revealed that a hoof does not hit the ground in a flat position, even when the heel and toe are indeed horizontally aligned. In accordance with results of other kinetic studies and point-of-zero moment analysis,[36,37] impact at landing was invariably on the lateral aspect of the hoof for all horses. At the beginning of the stance phase, the limb was globally adducted, resulting in a preferential exposition of the lateral aspect of the hoof at impact. This was consequently followed by a medial rocking motion of the hoof during landing until the hoof was flat and stabilized.

Three-dimensional kinematics of the hoof have been documented in a study[38] in which investigators had tools that are used to determine an aircraft's position and attitude relative to the ground. They measured pitch, roll, and yaw angles of the hooves in trotting horses, but they did not provide information on the hooves during landing, and 3-D motion of the hooves was not related to 3-D joint motion. The study reported here documented that changes in the mediolateral orientation of a hoof during landing unequivocally affect extrasagittal motions of the digital joints. Both the PIPJ and DIPJ underwent medial rotation associated with the medial rocking motion of the hoof, and the DIPJ concurrently underwent lateromotion (ie, narrowing of the articular space laterally on the side of the hoof that hit the ground first). Interestingly, medial rotation and lateromotion of the DIPJ were coupled, which has been observed during asymmetric loading of isolated forelimbs in other studies.[2,8]

Patterns of flexion-extension of the MPJ and DIPJ have been described in other kinematic studies[39-41] in walking horses by use of external landmarks or skin markers. However, those studies were limited to kinematics in the sagittal plane, and calculation of MPJ and DIPJ angles was distorted by the assumption that the proximal and middle phalanges could be considered as a rigid segment. Analysis of results of the study reported here documented that the range of flexion and extension of the PIPJ cannot be neglected and should be included in biomechanical models of the distal portion of the forelimbs of horses. In horses walking in a straight line, the PIPJ underwent approximately 5% of the entire interphalangeal flexion and 24% of the extension (10° for the PIPJ versus 42.4° for the DIPJ). The substantial involvement of the PIPJ in this movement could explain why arthrodesis of the PIPJ is sometimes followed by a worsening of navicular conditions.[42] Some studies[43-45] have reported sagittal movements of the PIPJ by use of skin markers in trotting horses, but the authors of those studies emphasized that skin displacement relative to the PIPJ has not been investigated, and correction algorithms were not available for this anatomic site. In 1 study,[43] it was reported that the amplitude of PIPJ flexion was approximately 10° and extension approximately 35° during the stance phase during trotting. but it is likely that skin markers may not represent actual movements of the underlying bones because accurate placement of the markers on the center of rotation of a joint is particularly difficult,[45] and skin displacement artifacts may be of a large magnitude in this area.[6]

Maximal flexion of the PIPJ and DIPJ was substantially earlier than maximal extension of the MPJ (13.7% and 20.0% of the stance phase for the PIPJ and DIPJ, respectively, vs 39.7% of the stance phase for the MPJ). The interphalangeal joints began to extend and, consequently, to raise the distal condyles of the third metacarpal bone while the MPJ continued to extend; thus, the decrease of the altitude of the distal condyles of the third metacarpal bone should not be confused with extension of the MPJ.

Extension of the MPJ was associated with lateral rotation of the joint, whereas flexion was associated with medial rotation. These results are in accordance with those of an in vitro study[9] and corroborate anatomic and functional observations.[46] However, these results depend on the choice of the anatomic axes. Considering that the discrepancy between in vivo and in vitro calibrations was maximal for the axial rotation angle of the MPJ, results must be interpreted with caution because of possible cross-talk drift.

In horses walking in a straight line on a hard track, extrasagittal movements of the digital joints were mainly during landing and breakover because of changes in the transverse orientation of the hoof. The involvement of the PIPJ was substantial, especially with axial rotation movements. Analysis of this result confirms that the PIPJ plays an important role in extrasagittal balance of the distal portion of the forelimb. These 3-D motions, coupled with asymmetric landing of the hoof at impact, should be taken into account to explain concussion of the joints and subsequent pain, even when a horse is walking in a straight line. It is likely that axial rotation movements are higher for horses during turns and at high speeds. To our knowledge, the study reported here provides the first set of 3-D data for the distal portion of the forelimb that will be useful for comparing the effects of movement (circle vs straight line), ground surface properties (sand track vs hard track), and interactions with various therapeutic shoes in moving horses.

[a]4-mm Schanz screw, Fixomed, Banyuls sur Mer, France.
[b]CMS-HS, Zebris Medizintechnik GmbH, Isny, Germany.
[c]Windata, version 19.31, Zebris Medizintechnik GmbH, Isny, Germany.
[d]TS-U1, Zebris Medizintechnik GmbH, Isny, Germany.
[e]Matlab, The MathWorks, Natick, Mass.

References

1. Aoki O. Biomechanical analysis of horse shoeing. *Equine Vet J Suppl* 1999;30:629–630.

2. Denoix J. Functional anatomy of the equine interphalangeal joints, in *Proceedings*. Am Assoc Equine Pract 1999;174–177.

Unauthenticated | Downloaded 10/03/22 08:51 AM UTC

3. Willemen MA, Savelberg HHCM, Barneveld A. The effect of orthopaedic shoeing on the force exerted by the deep digital flexor tendon on the navicular bone in the horses. *Equine Vet J* 1999; 31:25–30.

4. Scheffer CJ, Back W. Effects of 'navicular' shoeing on equine distal forelimb kinematics on different track surface. *Vet Q* 2001; 23:191–195.

5. Balch O, White K. Lameness associated with severe fetlock synovitis managed by balanced trimming and shoeing. *Equine Pract* 1985;7:35–40.

6. Crevier-Denoix N, Roosen C, Dardillat C, et al. Effects of heel and toe elevation upon the digital joint angles in the standing horse. *Equine Vet J Suppl* 2001;33:74–78.

7. Van Weeren PR, Barneveld A. A technique to quantify skin displacement in the walking horse. *J Biomech* 1986;19:879–883.

8. Chateau H, Degueurce C, Jerbi H, et al. Three-dimensional kinematics of the equine interphalangeal joints: articular impact of asymmetric bearing. *Vet Res* 2002;33:371–382.

9. Chateau H, Degueurce C, Jerbi H, et al. Normal three-dimensional behaviour of the metacarpophalangeal joint and the effect of uneven foot bearing. *Equine Vet J Suppl* 2001;33:84–88.

10. Caudron I, Grulke S, Farnir F, et al. Radiographic assessment of equine interphalangeal joints asymmetry: articular impact of phalangeal rotations (part 1). *Zentralbl Veterinarmed [A]* 1998;45:319–325.

11. Riemersma DJ, van den Bogert AJ, Schamhardt HC, et al. Kinetics and kinematics of the equine hind limb: in vivo tendon strain and joint kinematics. *Am J Vet Res* 1988;49:1353–1359.

12. Jansen MO, Buiten A, van den Bogert AJ, et al. Strain of the Musculus interosseus medius and its Rami extensorii in the horse, deduced from in vivo kinematics. *Acta Anat (Basel)* 1993;147:118–124.

13. Degueurce C, Chateau H, Jerbi H, et al. Three-dimensional kinematics of the proximal interphalangeal joint: effects of raising the heels or the toe. *Equine Vet J Suppl* 2001;33:79–83.

14. Bushe T, Turner TA, Poulos PW, et al. The effect of hoof angle on coffin, pastern and fetlock joint angles, in *Proceedings*. Am Assoc Equine Pract 1987;729–738.

15. Cappozzo A, Catani F, Croce UD, et al. Position and orientation in space of bones during movement: anatomical frame definition and determination. *Clin Biomech (Bristol, Avon)* 1995;10:171–178.

16. Grood ES, Suntay WJ. A joint coordinate system for the clinical description of three-dimensional motions: application to the knee. *J Biomech Eng* 1983;105:136–144.

17. Degueurce C, Chateau H, Pasqui-Boutard V, et al. Concrete use of the joint coordinate system for the quantification of articular rotations in the digital joints of the horse. *Vet Res* 2000;31:297–311.

18. Chateau H, Girard D, Degueurce C, et al. Methodological considerations for using a kinematic analysis system based on ultrasonic triangulation. *ITBM-RBM Innovation et Technologie en Biologie et Médecine* 2003;24:69–78.

19. Drevemo S, Dalin G, Fredricson I, et al. Equine locomotion: 1. The analysis of linear temporal stride characteristics of trotting Standardbreds. *Equine Vet J* 1980;12:60–65.

20. Lanovaz JL, Khumsap S, Clayton HM, et al. Three-dimensional kinematics of the tarsal joint at the trot. *Equine Vet J Suppl* 2002;34:308–313.

21. Selvik G. Roentgen stereophotogrammetry. *Acta Orthop Scand* 1989;60:1–51.

22. Wu G, Cavanagh PR. ISB recommendations for standardization in the reporting of kinematic data. *J Biomech* 1995;28:1257–1261.

23. Chao EYS. Justification of triaxial goniometer for the measurement of joint rotation. *J Biomech* 1980;13:989–1006.

24. Fuller J, Liu L, Murphy MC, et al. A comparison of lower-extremity skeletal kinematics measured using skin- and pin-mounted markers. *Hum Mov Sci* 1997;16:219–242.

25. Ramsey DK, Wretenberg PF. Biomechanics of the knee: methodological considerations in the in vivo kinematic analysis of the tibiofemoral and patellofemoral joint. *Clin Biomech (Bristol, Avon)* 1999;14:595–611.

26. Ramsey DK, Lamontagne M, Wretenberg PF, et al. Assessment of functional knee bracing: an in vivo three-dimensional kinematic analysis of the anterior cruciate deficient knee. *Clin Biomech (Bristol, Avon)* 2001;16:61–70.

27. Lafortune MA, Cavanagh PR, Sommer HJ, et al. Three-dimensional kinematics of the human knee during walking. *J Biomech* 1992;25:347–357.

28. Reinschmidt C, van den Bogert AJ, Lundberg A, et al. Tibiofemoral and tibiocalcaneal motion during walking: external vs. skeletal markers. *Gait Posture* 1997;6:98–109.

29. Dyhre-Poulsen P, Smedegaard HH, Roed J, et al. Equine hoof function investigated by pressure transducers inside the hoof and accelerometers mounted on the first phalanx. *Equine Vet J* 1994; 26:362–366.

30. Korvick DL, Pijanowski GJ, Schaeffer DJ. Three-dimensional kinematics of the intact and cranial cruciate ligament-deficient stifle of dogs. *J Biomech* 1994;27:77–87.

31. Van Dixhoorn ID, Meershoek LS, Huiskes R, et al. A description of the motion of the navicular bone during in vitro vertical loading of the equine forelimb. *Equine Vet J* 2002;34:594–597.

32. Ramakrishnan HK, Kadaba MP. On the estimation of joint kinematics during gait. *J Biomech* 1991;24:969–977.

32. Willemen MA, Savelberg HHCM, Bruin G, et al. The effect of toe weights on linear and temporal stride characteristics of standardbred trotters. *Vet Q* 1994;16:97–100.

34. Clayton HM. The effect of an acute hoof wall angulation on the stride kinematics of trotting horses. *Equine Vet J Suppl* 1990; 9:86–90.

35. Schamhardt HC, Merkens HW. Objective determination of ground contact of equine limbs at the walk and trot: comparison between ground reaction forces, accelerometer data and kinematics. *Equine Vet J Suppl* 1994;17:75–79.

36. Eliashar E, McGuigan MP, Rogers KA, et al. A comparison of three horseshoeing styles on the kinetics of breakover in sound horses. *Equine Vet J* 2002;34:184–190.

37. Wilson AM, Seelig TJ, Shield RA, et al. The effect of hoof imbalance on point of force application in the horse. *Equine Vet J* 1998; 30:540–545.

38. Fredricson I, Drevemo S. A new method of investigating equine locomotion. *Equine Vet J* 1971;3:137–140.

39. Hodson E, Clayton HM, Lanovaz JL. The forelimb in walking horses: 1. Kinematics and ground reaction forces. *Equine Vet J* 2000; 32:287–294.

40. Back W, Schamhardt HC, Barneveld A. Are kinematics of the walk related to the locomotion of a warmblood horse at the trot? *Vet Q* 1996;18:79–85.

41. Colborne GR, Lanovaz JL, Sprigings EJ, et al. Forelimb joint moments and power during the walking stance phase of horses. *Am J Vet Res* 1998;59:609–614.

42. Martin GS, McIlwraith CW, Turner AS, et al. Long-term results and complications of proximal interphalangeal arthrodesis in horses. *J Am Vet Med Assoc* 1984;184:1136–1140.

43. Clayton HM, Singleton WH, Lanovaz JL, et al. Sagittal plane kinematics and kinetics of the pastern joint during the stance phase of the trot. *Vet Comp Orthop Traumatol* 2002;15:15–17.

44. Roepstorff L, Johnston C, Drevemo S. The effect of shoeing on kinetics and kinematics during the stance phase. *Equine Vet J Suppl* 1999;30:279–285.

45. Drevemo S, Johnston C, Roepstorff L, et al. Nerve block and intra-articular anaesthesia of the forelimb in the sound horse. *Equine Vet J Suppl* 1999;30:266–269.

46. Rooney JR. Individual joints of the forelimb. In: Rooney JR, ed. *Biomechanics of lameness in horses*. Baltimore: The Williams & Wilkins Co, 1969;69–78.

Unauthenticated | Downloaded 10/03/22 08:51 AM UTC